NASA TM X-83

TECHNICAL MEMORANDUM

X-83

OVEREXPANDED PERFORMANCE OF CONICAL NOZZLES WITH AREA RATIOS OF 6 AND 9 WITH AND WITHOUT SUPERSONIC EXTERNAL FLOW

Norman T. Musial and James J. Ward

Lewis Research Center
Cleveland, Ohio

CLASSIFIED DOCUMENT - TITLE UNCLASSIFIED

NATIONAL AERONAUTICS AND SPACE ADMINISTRATION

WASHINGTON September 1959

CRV

[illegible]

copy #1

NATIONAL AERONAUTICS AND SPACE ADMINISTRATION

TECHNICAL MEMORANDUM X-83

OVEREXPANDED PERFORMANCE OF CONICAL NOZZLES WITH AREA RATIOS OF 6 AND 9 WITH AND WITHOUT SUPERSONIC EXTERNAL FLOW*

By Norman T. Musial and James J. Ward

SUMMARY

An investigation of the thrust characteristics and internal pressure distributions of two convergent-divergent 15° half-angle exhaust nozzles having area ratios of 6 and 9 was made in the NASA Lewis 10- by 10-foot supersonic wind tunnel. The tests were conducted at free-stream Mach numbers of 0, 2.0, 2.5, 3.0, and 3.5 over a range of nozzle pressure ratios from 3 to 105. Attempts were made to induce separation of the overexpanded nozzle flow using secondary airflow and a wedge.

Nozzle flow expansion under all free-stream conditions followed one-dimensional theory until separation from the nozzle wall occurred. In quiescent air the nozzle flow expanded to a pressure approximately one-half the base pressure before separation. When the nozzles were tested with supersonic external flow at the same effective pressure ratios, the nozzle flow separated with negligible expansion below the base pressure. The effect of a supersonic stream on internal nozzle flow separation characteristics was well defined only at a free-stream Mach number of 2.0.

Thrust data at supersonic free-stream conditions indicate that only a small percentage of the ideal nozzle thrust will be available at nozzle pressure ratios below design. However, the overexpanded primary nozzle thrust loss was decreased by injecting large quantities of secondary air near the nozzle exit. In most cases no net gain in thrust resulted from secondary-air injection when the nozzle thrust was compared with the ideal thrust of both the primary and secondary airflows.

INTRODUCTION

For the nozzle pressure ratios available with air-breathing engines at Mach numbers greater than 2.0, it is advantageous to expand the flow in a convergent-divergent exhaust nozzle. The thrust to be gained by expanding the nozzle flow increases with nozzle pressure ratio; however, the performance of these nozzles operating in the overexpanded region is poor.

*Title, Unclassified.

Quiescent air tests and wind tunnel tests (refs. 1 to 3) have indicated overexpansion of the flow in the nozzle at pressure ratios lower than design with a resultant thrust loss. In an effort to increase the off-design thrust, additional tests have been made (refs. 4 and 5) employing secondary air injection to induce separation in the nozzle.

The majority of data available, however, are for small-scale nozzles with area ratios on the order of 2 to 3. A very limited amount of data exists for the off-design performance of large-scale convergent-divergent nozzles in a supersonic stream. Consequently, a test program was conducted in the Lewis 10- by 10-foot supersonic wind tunnel to determine the off-design performance of 15° half-angle conical nozzles with area ratios of 6 and 9 (designated herein as area ratio 6 and area ratio 9 nozzles). In addition, methods of increasing off-design thrust were studied.

This report presents the internal pressure distribution and thrust characteristics of the nozzles over a range of pressure ratios from 3 to 105 with free-stream Mach numbers of 0, 2.0, 2.5, 3.0, and 3.5. Also included are results of attempts to increase off-design nozzle performance by secondary-air injection and by mechanical means.

SYMBOLS

A	internal flow area, sq ft
F	nozzle jet thrust, $mV_t + (p_t - p_0)A_t + \int_{A_t}^{A_e} (p - p_0)dA$, lb
F_i	ideal nozzle jet thrust, mV_e
(F/F_i)	thrust ratio
M	Mach number
m	mass flow
P	total pressure
p	static pressure
V	velocity
w	airflow

Subscripts:

b	base
c	nozzle entrance
e	nozzle exit
i	ideal
l	local
p	primary
s	secondary
t	nozzle throat
0	free stream

APPARATUS AND PROCEDURE

A schematic diagram of the jet-exit model installed in the 10- by 10-foot supersonic wind tunnel is presented in figure 1. Primary and secondary air were supplied from a central high-pressure laboratory source and introduced into the model through passages in the support strut. The two air supplies were individually throttled by control valves to the desired operating pressure. Airflows were measured with standard ASME sharp-edged orifice plates ahead of the control valves. Air entering the model was maintained at a temperature of approximately 500° R and a dewpoint of -20° to -30° F.

Details of the nozzle configurations investigated are presented schematically in figure 2. Both nozzles had a 15° conical divergent section faired to the throat by a circular arc. Nozzle 1 (fig. 2(a)) had an area ratio of 6, a throat diameter of 5.42 inches, and an on-design nozzle pressure ratio of 63.2. Nozzle 2 (fig. 2(b)) had an area ratio of 9, a throat diameter of 4.39 inches, and an on-design nozzle pressure ratio of 117. The on-design nozzle pressure ratios were calculated on the basis of gamma equal to 1.4.

Internal nozzle pressure instrumentation consisted of two rows of static-pressure orifices located on the top and bottom of the nozzles extending from the throat to the nozzle exit. Base pressures were measured by static-pressure orifices located at the base annulus of the model.

The two regions indicated in figure 2(a) and the three regions indicated in figure 2(b) represent areas of nozzle secondary air injection. In each region, secondary air was admitted through ninety 3/16-inch-diameter holes. The holes were arranged in a spiral pattern to ensure full coverage of the injection area and were drilled perpendicular to the nozzle centerline. Secondary air was admitted through only one of the regions in the nozzle at any given time. During the basic nozzle tests the holes were filled.

In figure 2(c) the shaded area indicates the position of an annular wedge inserted in the divergent portion of the area ratio 6 nozzle. The axial location of the wedge was approximately the same as the upstream secondary air injection region of the nozzle.

Nozzle thrust was determined by the pressure integration technique (ref. 3). In this method, the nozzle thrust is divided into two parts: the theoretical sonic thrust at the throat and the pressure-area contribution of the divergent portion of the nozzle. The sonic thrust is calculated from the total momentum parameter at the throat assuming isentropic one-dimensional flow. The thrust increment due to the divergent portion of the nozzle is equal to the integration of local wall static pressure minus free-stream static pressure on the projected surface area. This thrust measurement technique neglects any nozzle friction forces.

The pressure integration technique was also employed for the case of secondary air injection near the nozzle exit. In this case, the area occupied by the injection holes was considered as contributing to the nozzle thrust. The amount of error introduced because some of the pressure measurements were made in the region of air injection is believed to be small. This technique could not be used with secondary air injection at the midstation or near the throat of the nozzle because of erratic indications of pressure in these areas.

Nozzle total pressure was calculated from static-pressure measurements at the nozzle entrance and from the Mach number at this station as determined from continuity relations. The nozzle mass-flow coefficient was on the order of 0.99 for both nozzles.

RESULTS AND DISCUSSION

Basic Nozzle Performance

The variation of nozzle pressure ratio with Mach number for a typical ramjet-powered vehicle is presented in figure 3. As is shown, the operating nozzle pressure ratio increases rapidly with free-stream

Mach number. From figure 3 it may also be seen that the area ratio 6 and 9 nozzles would be applicable for ramjet operation at Mach numbers of approximately 3.8 and 4.4, respectively.

Nozzle pressure distributions for the area ratio 9 nozzle at free-stream Mach numbers of 0 and 2.0 to 3.5 are presented in figure 4. With no external flow, the pressure distributions follow the anticipated quiescent air trends (fig. 4(a)). At pressure ratios well below design, the flow expands to a pressure that is approximately one-half the ambient base pressure and separates from the nozzle wall. The separation is accompanied by a pressure rise to the base pressure.

Supersonic external flow causes a reduction in the nozzle base pressure resulting in an increase in the pressure ratio across the nozzle. As long as the pressure ratio is sufficiently high to maintain unseparated flow throughout the nozzle, the internal pressure distribution is the same for all external Mach numbers and is close to the one-dimensional pressure distribution (figs. 4(b) to (e)).

With Mach 2.0 external flow (fig. 4(b)), pressure ratios low enough to cause separation were investigated. Here the nozzle flow expanded essentially only to base pressure and separated from the nozzle wall at that value. It appears that for the range of nozzle pressure ratios between 6.7 and 19.0, separation may have occurred at an upstream point in the nozzle followed by an immediate reattachment and further expansion. It may also be seen from figure 4(b) that as the pressure ratio increases from 6.7, the pressure distribution curves upstream of the point of final separation approach the one-dimensional curve. Beyond a pressure ratio of 19, however, there is no further reduction of the local pressure ratio value. This phenomenon is well-defined only with Mach 2.0 external flow.

Since the nozzle performance is strongly influenced by the pressure existing at the nozzle exit, data for a given nozzle pressure ratio in quiescent air may be compared with data in a supersonic stream at the same effective pressure ratio. The effective pressure ratio in a supersonic stream is the ratio of nozzle total pressure to base pressure. Thus, the curve for the square symbols in figure 4(b), (P_c/p_b = 11.1) may be compared with the curve for the circle symbols of figure 4(a) (P_c/p_0 = 11.8). This comparison indicates more overexpansion of the nozzle flow for the data at quiescent conditions than in a supersonic stream at the same effective pressure ratio. Unpublished NASA data from a subsequent test with an area ratio 8 nozzle in a supersonic stream indicate that a random pressure oscillation having an amplitude of approximately twice the local nozzle static pressure occurs near the point of separation. Such shock fluctuations may be the cause of the marked difference in separation characteristics.

The ratio of thrust determined by the pressure integration technique to the ideal thrust for the area ratio 9 nozzle is presented in figure 5(a) as a function of nozzle pressure ratio for a range of free-stream Mach numbers. The thrust ratios with supersonic external flow agree with the values predicted by one-dimensional flow theory since the nozzle flow follows one-dimensional expansion over the pressure ratio range for which thrust data are presented. The thrust ratios for pressure ratios below design are extremely low. For example, at a free-stream Mach number of 2.0 at which a ramjet operating pressure ratio of 6.0 would be available the thrust ratio is about 0.15.

Quiescent-air thrust ratios are higher than the corresponding thrust ratios obtained in a supersonic stream. In the latter case the decreased base pressure causes the nozzle to operate greatly over-expanded thereby increasing the thrust loss.

Thrust data for the area ratio 6 nozzle are presented in figure 5(b) for a range of nozzle pressure ratios and free-stream Mach numbers. Again, the thrust ratio follows that predicted by one-dimensional flow theory over the range investigated. In this case, at a free-stream Mach number of 2.0 with a corresponding nozzle pressure ratio of 6.0, the thrust ratio is 0.60, indicating a much higher off-design thrust than for the area ratio 9 nozzle. This occurs because the area ratio 6 nozzle is operating closer to design pressure ratio at this condition. As with the area ratio 9 nozzle the quiescent air thrust ratios are higher than the comparable data obtained with supersonic external flow.

Nozzle Performance With Induced Flow Separation

Both mechanical and aerodynamic methods were employed to induce nozzle flow separation at supersonic free-stream Mach numbers. The mechanical method involved the insertion of a metal wedge at approximately the Mach 2.0 station in the area ratio 6 nozzle (fig. 2(c)). This disturbance, however, appeared to have little effect, as the nozzle flow reattached to the wall of the nozzle a short distance downstream of the wedge.

The aerodynamic method of inducing separation involved the use of secondary air injection. Secondary air was injected into three regions of the area ratio 9 nozzle and into two regions of the area ratio 6 nozzle as indicated in figure 2. Typical nozzle pressure distribution data obtained with secondary air injection in the area ratio 9 nozzle are presented in figure 6 for a nozzle pressure ratio of approximately 10.0 and a free-stream Mach number of 2.5. Also included for comparison are the pressure distribution data for no secondary flow. When air was injected near the nozzle throat (fig. 6(a)), some increase in

static pressure was obtained near the region of injection indicating a small thrust increase. Air injection midway along the divergent portion of the nozzle (fig. 6(b)) caused a local static pressure rise with some effect on the nozzle flow upstream of the area of injection. An accurate measure of the increase in thrust could not be made in either of these cases because of the erratic behavior of the static pressures in the injection areas.

The largest increases in nozzle static pressure, and therefore nozzle thrust, occurred when secondary air was injected near the nozzle exit. Injection in this region increased the nozzle static pressure over a large portion of the nozzle upstream of the point of injection (fig. 6(c)). Nozzle thrust was calculated for this configuration using the integration method.

The thrust ratios obtained with secondary air injected near the exit are presented in figure 7 for the area ratio 9 nozzle as a function of secondary airflow. Since the air-injection area was fixed, the secondary airflow was controlled by varying the secondary-air chamber pressure. The ratio of secondary to primary chamber pressure reached a value of 1.0 at an airflow ratio w_s/w_p of 0.175 and a maximum value of 3.7 at an airflow ratio of 0.63. For the case in which the nozzle jet thrust is compared with the ideal primary nozzle thrust $F_{i,p}$, it is shown that an increase in thrust ratio occurs for all nozzle pressure ratios; however, the rate of increase of thrust ratio with secondary airflow decreases with increasing nozzle pressure ratio. Conversely the thrust ratios obtained by including the ideal secondary airflow thrust $F_{i,s}$, in most cases decrease with increasing nozzle pressure ratio. In only one instance, $M = 2.0$ and $P_c/p_0 = 7.0$, did the value of this ratio exceed the value obtained with no secondary airflow.

The variation in thrust ratio slope occurs because of the difference in separation characteristics between the high and low nozzle pressure ratios. Air injection at low nozzle pressure ratio has the effect of inducing separation of the nozzle flow at pressures near the exit base pressure, as is shown in figure 6(c). This phenomena is probably similar to that observed at even lower nozzle pressure ratios with no secondary airflow (fig. 4(b)). At the higher nozzle pressure ratios, the nozzle flow separates in a manner similar to that observed with the nozzle in quiescent air; that is, the nozzle flow expands below the exit base pressure before separating from the nozzle wall. It is also observed that, at the lower nozzle pressure ratios with no secondary airflow, the nozzle with injection holes open has a higher thrust ratio than the nozzle with these holes filled.

CONCLUDING REMARKS

From an experimental investigation of two convergent-divergent exhaust nozzles having area ratios of 6 and 9 the following observations can be made:

The nozzle flow expansion followed one-dimensional flow theory over most of the nozzle pressure ratio range when the nozzles were operating in a supersonic stream.

At pressure ratios well below design, quiescent air data indicate that the nozzle flow overexpands below base pressure. This overexpansion is followed by a pressure rise to the base pressure. Nozzle data with Mach number 2.0 external flow at the same effective nozzle pressure ratio (in this case calculated from the base pressure) indicate that the nozzle flow separates from the nozzle wall with negligible expansion below the base pressure.

During operation at nozzle pressure ratios below design in a supersonic stream, the overexpanded primary nozzle thrust loss was decreased by injection of large quantities of secondary air at the nozzle exit. In most cases, no net gain in thrust resulted from secondary-air injection when the nozzle thrust was compared with the ideal thrust of both the primary and secondary airflows.

Lewis Research Center
National Aeronautics and Space Administration
Cleveland, Ohio, May 1, 1959

REFERENCES

1. Fletcher, P. J.: Measurements of Thrust from Convergent-Divergent Propelling Nozzles. Memo. M.144, British NGTE, Feb. 1952.

2. Ashwood, P. F., Crosse, G. W., and Goddard, Jean E.: Measurements of the Thrust Produced by Convergent-Divergent Nozzles at Pressure Ratios up to 20. CP 326, British ARC, 1957.

3. Fradenburgh, Evan A., Gorton, Gerald C., and Beke, Andrew: Thrust Characteristics of a Series of Convergent-Divergent Exhaust Nozzles at Subsonic and Supersonic Flight Speeds. NACA RM E53L23, 1954.

4. Reshotko, Eli: Preliminary Investigation of a Perforated Axially Symmetric Nozzle for Varying Nozzle Pressure Ratios. NACA RM E52J27, 1953.

5. Foster, Charles R., and Cowles, Frederick B.: Experimental Study of Gas-Flow Separation in Overexpanded Exhaust Nozzles for Rocket Motors. Prog. Rep. 4-103, Jet Prop. Lab., C.I.T., May 9, 1949. (Contract W-04-200-ORD-455.)

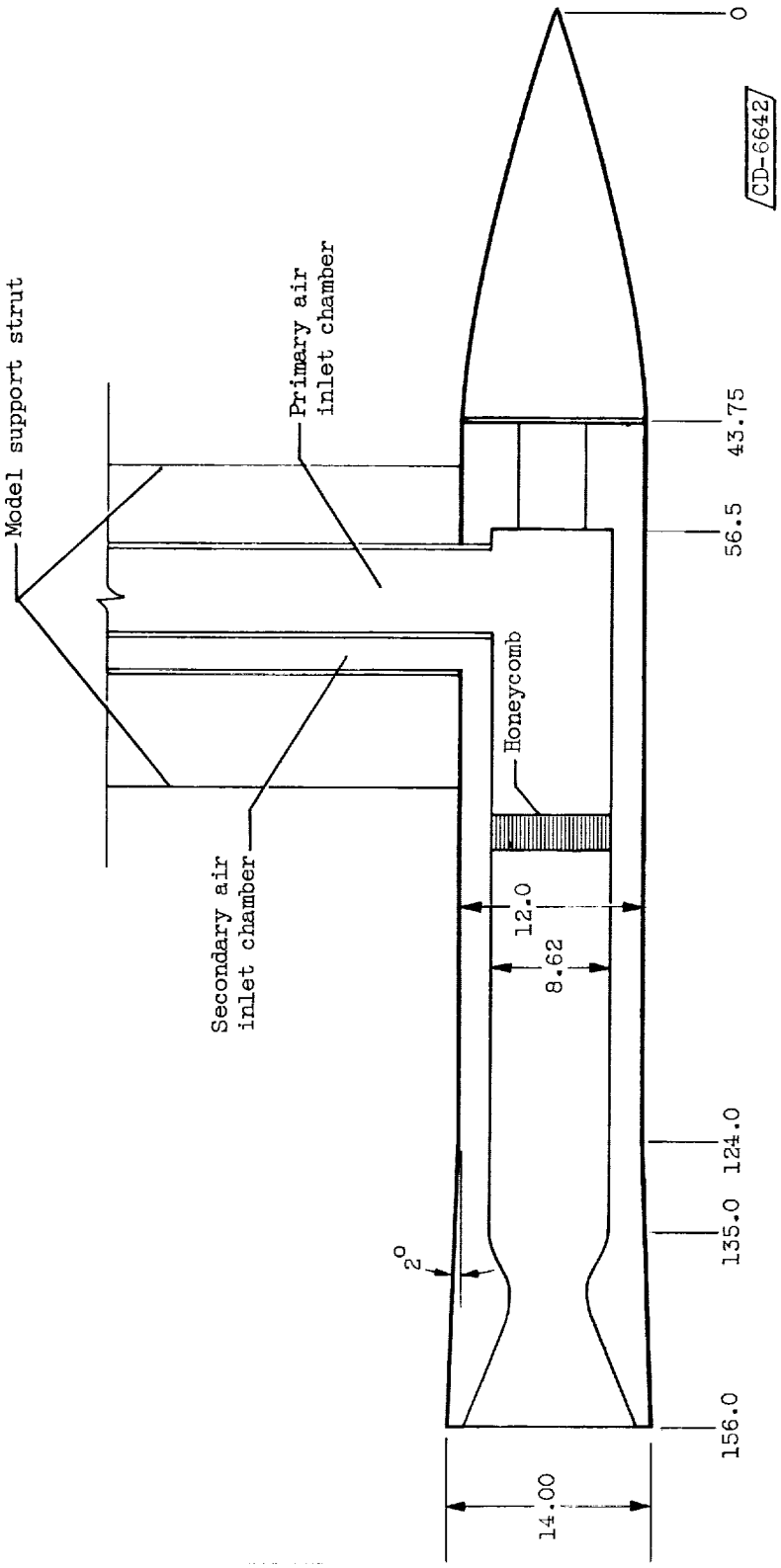

Figure 1. - Schematic diagram of jet-exit model. (Dimensions in inches.)

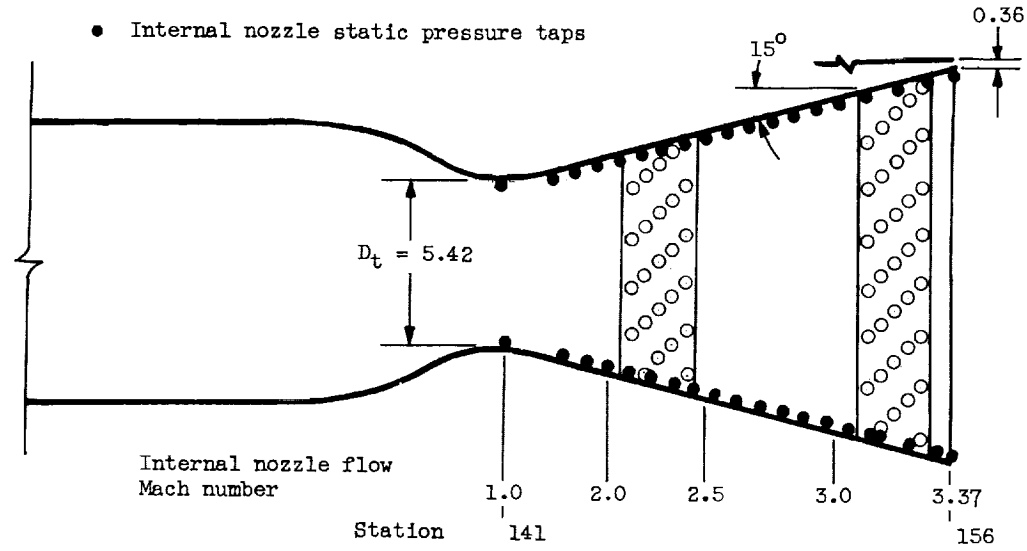

(a) Area ratio 6.0 nozzle.

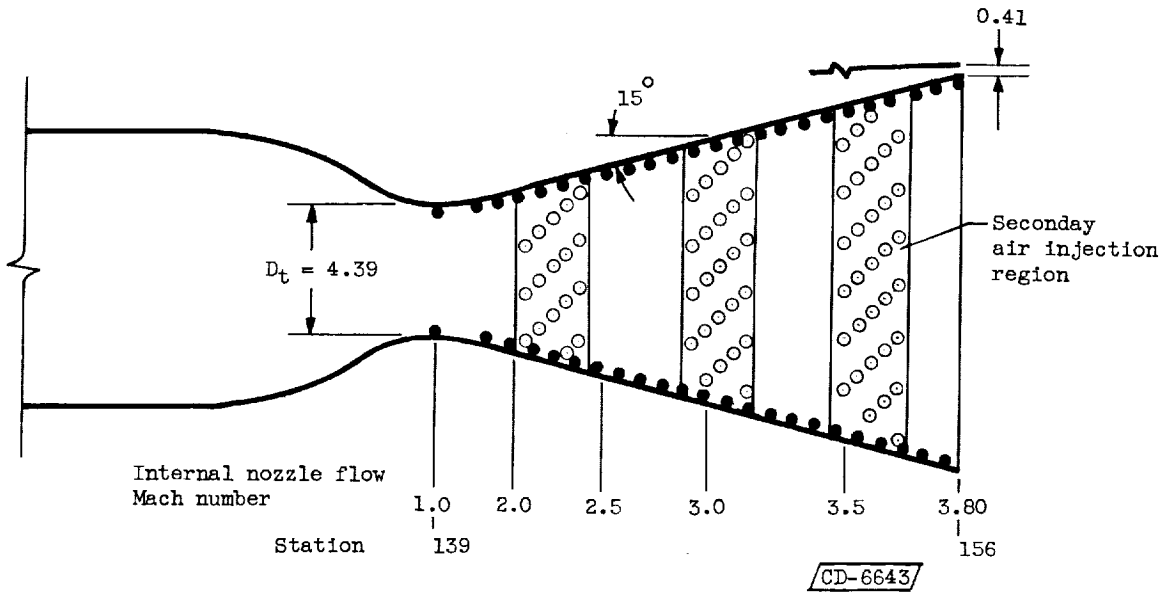

(b) Area ratio 9.0 nozzle.

Figure 2. - Schematic diagram of nozzles, including pressure instrumentation, secondary-air injection regions, and annular wedge position. (Dimensions in inches.)

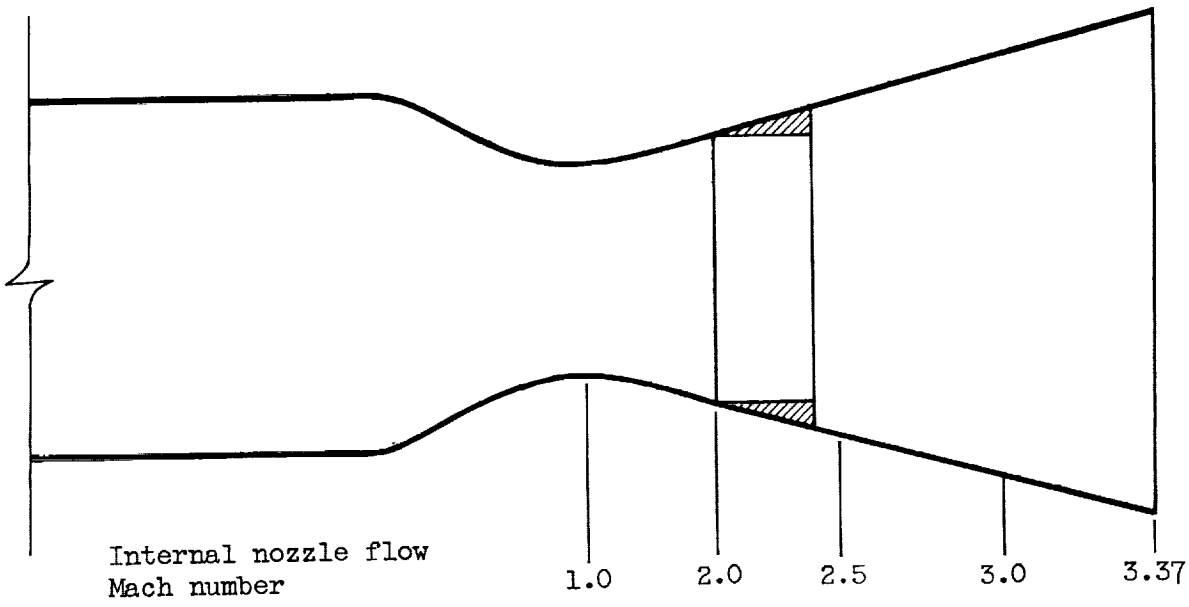

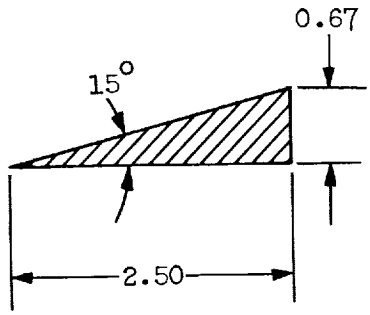

CD-6644

Detail of annular wedge insert

(c) Area ratio 6.0 nozzle with annular wedge inserted.

Figure 2. - Concluded. Schematic diagram of nozzles, including pressure instrumentation, secondary-air injection regions, and annular wedge position. (Dimensions in inches.)

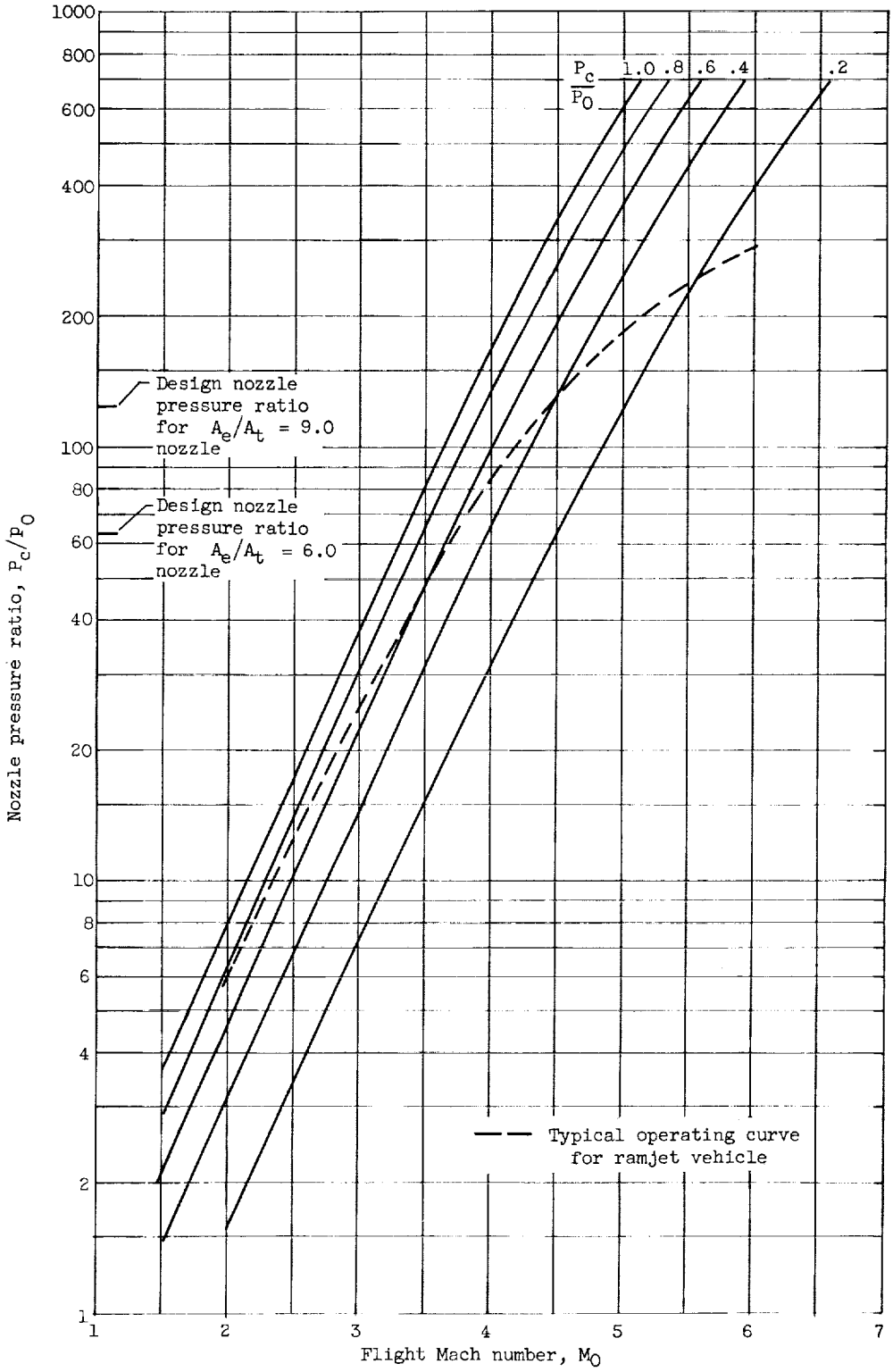

Figure 3. - Variation of nozzle pressure ratio with Mach number for a typical ramjet.

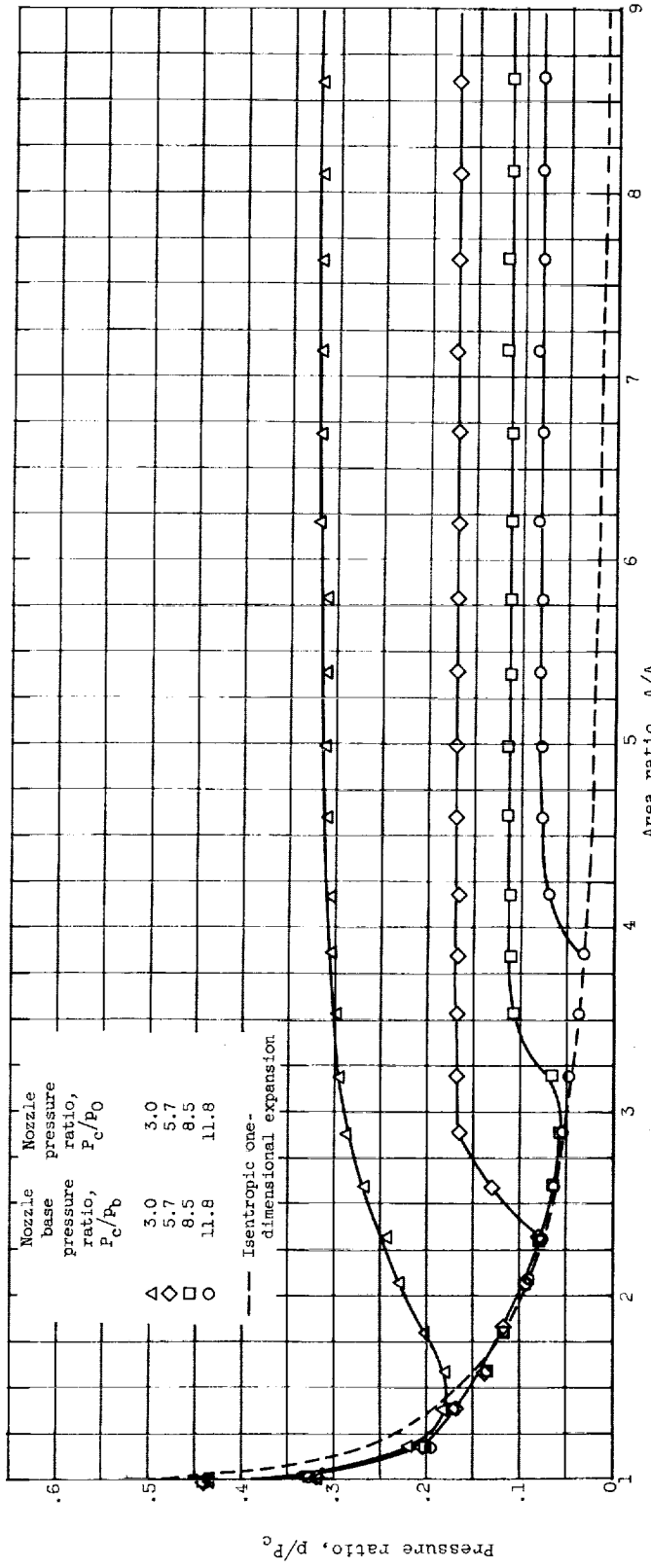

(a) Free-stream Mach number, zero; free-stream static pressure, 390 pounds per square foot.

Figure 4. - Nozzle pressure distributions for area ratio 9 nozzle.

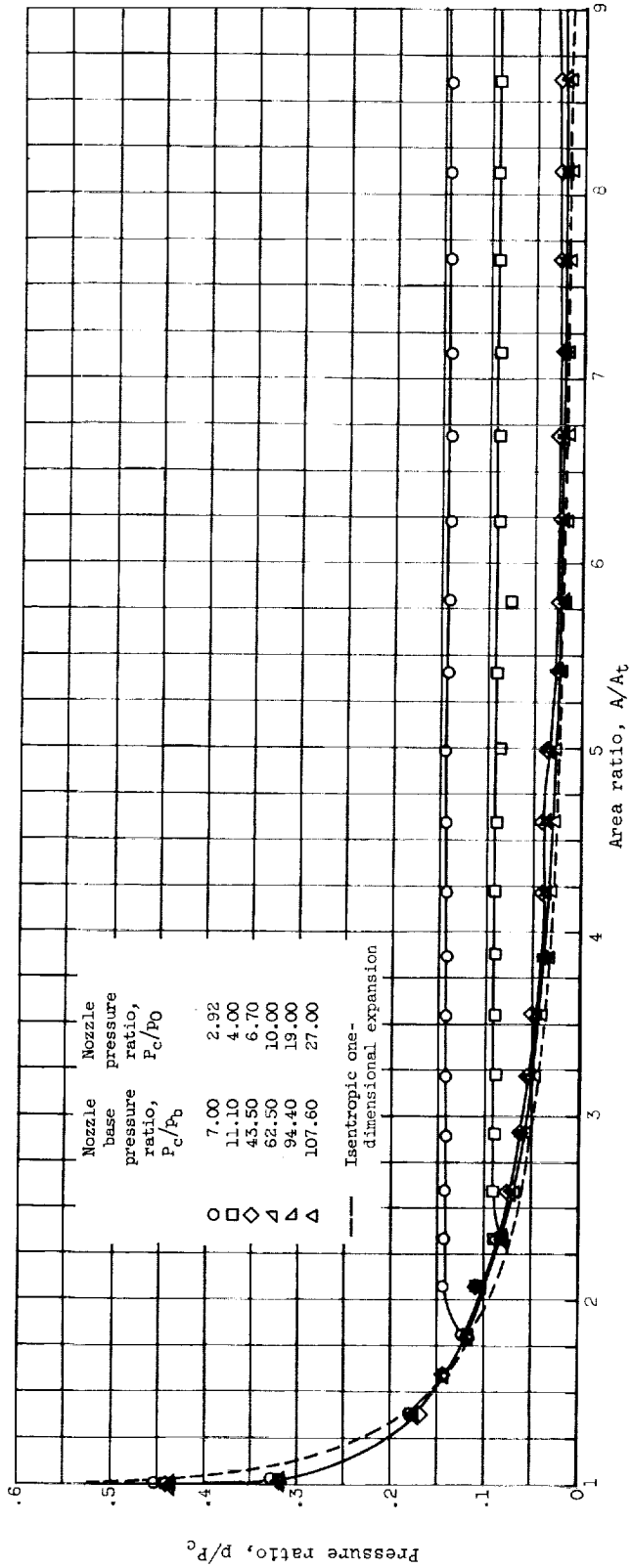

(b) Free-stream Mach number, 2.0; free-stream static pressure, 133 pounds per square foot.

Figure 4. - Continued. Nozzle pressure distributions for area ratio 9 nozzle.

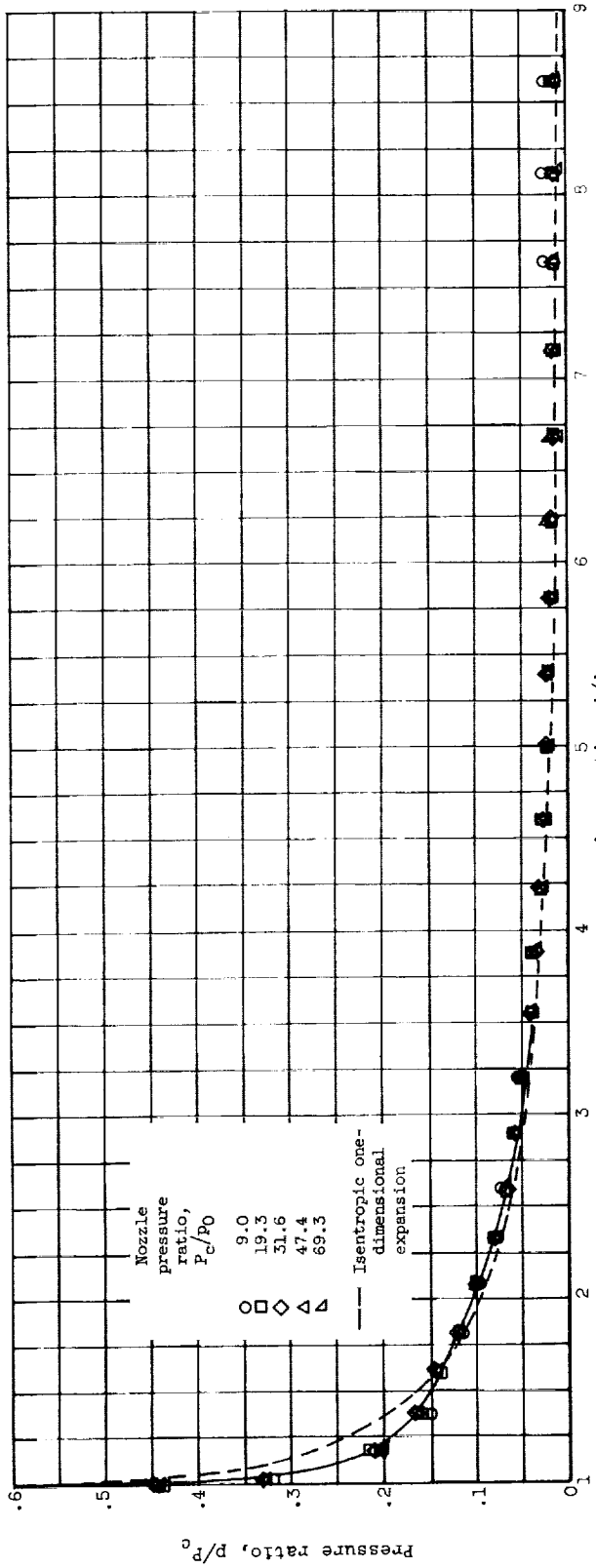

(c) Free-stream Mach number, 2.5; free-stream static pressure, 65 pounds per square foot.

Figure 4. - Continued. Nozzle pressure distributions for area ratio 9 nozzle.

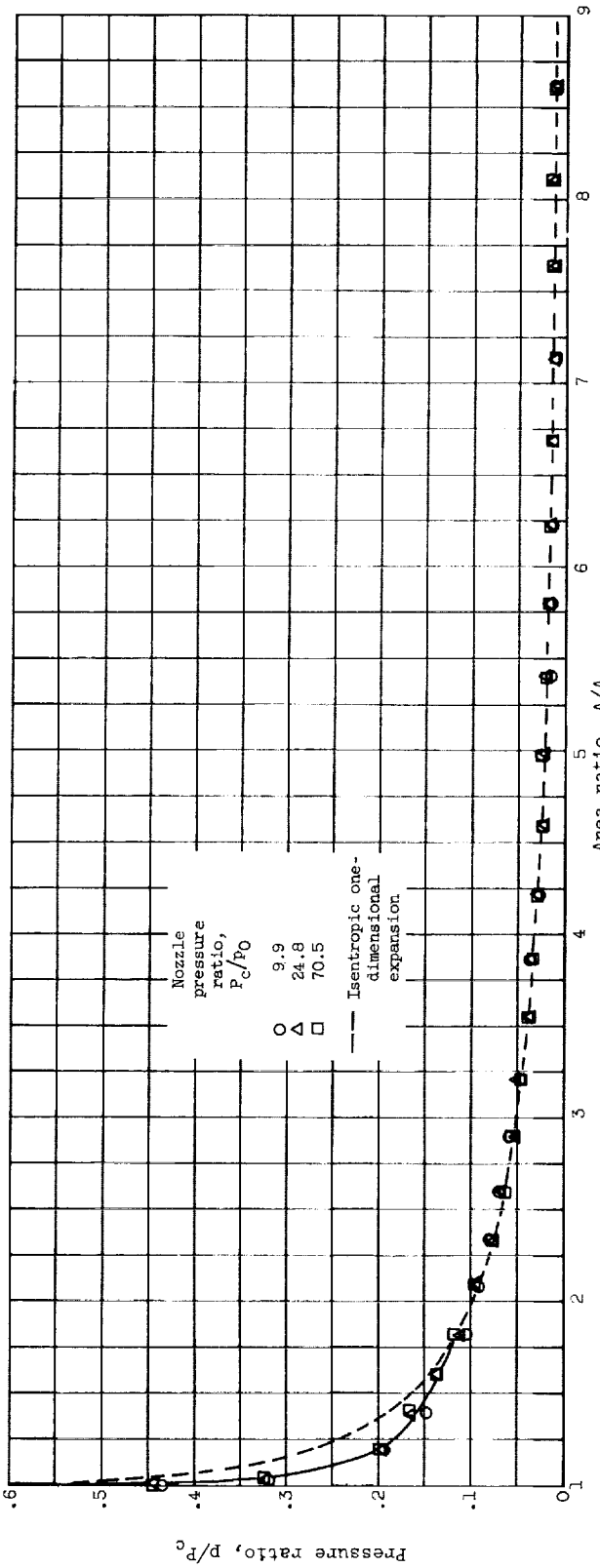

(d) Free-stream Mach number, 3.0; free-stream static pressure, 64 pounds per square foot.

Figure 4. - Continued. Nozzle pressure distributions for area ratio 9 nozzle.

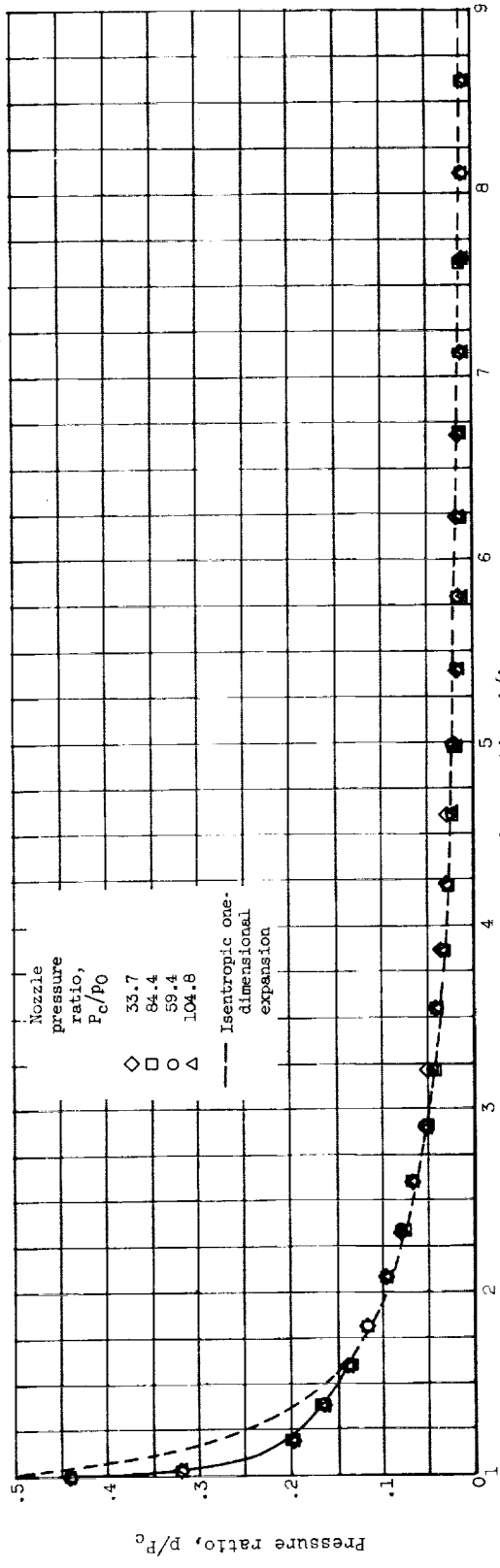

(e) Free-stream Mach number, 3.5; free-stream static pressure, 43 pounds per square foot.

Figure 4. - Concluded. Nozzle pressure distributions for area ratio 9 nozzle.

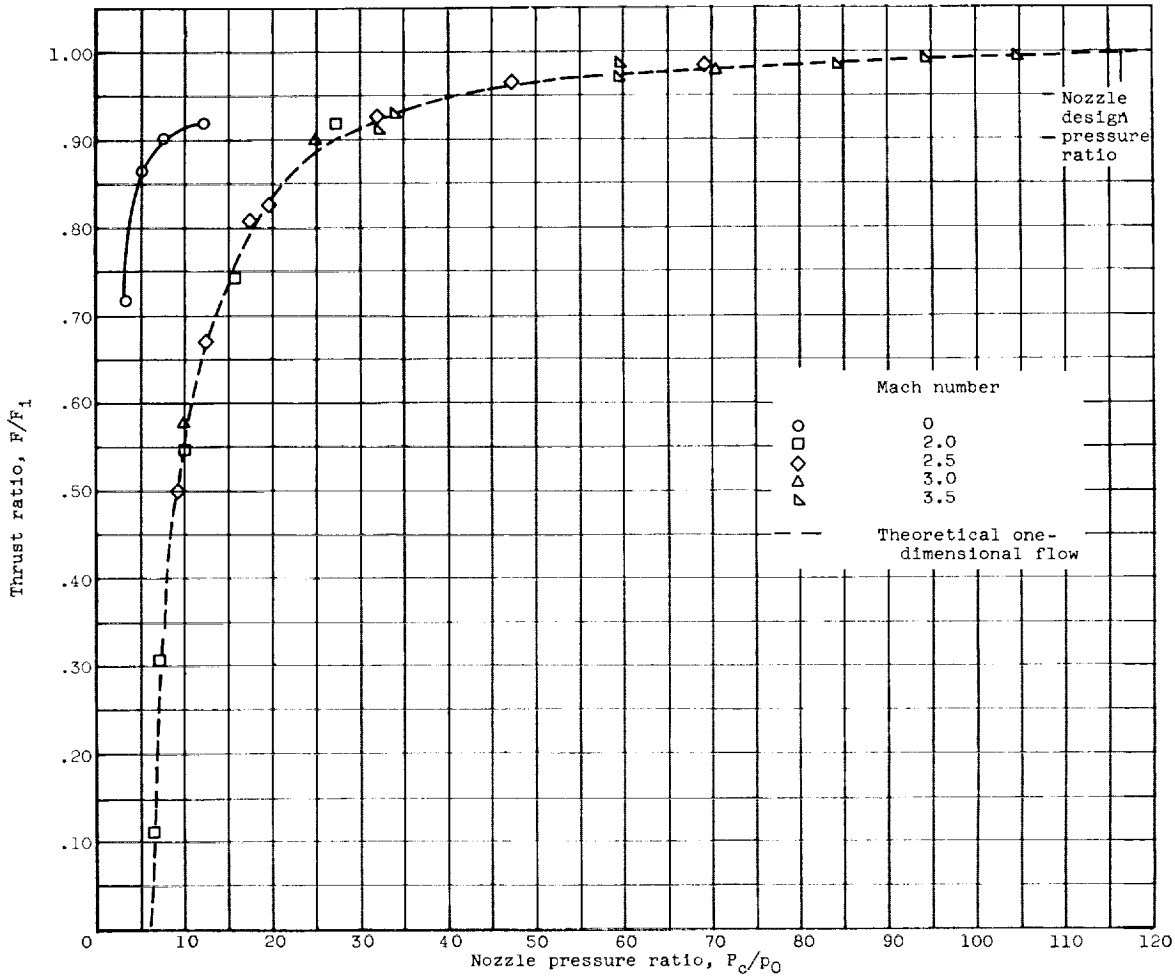

(a) Nozzle area ratio, 9.0.

Figure 5. - Variation of thrust ratio with nozzle pressure ratio.

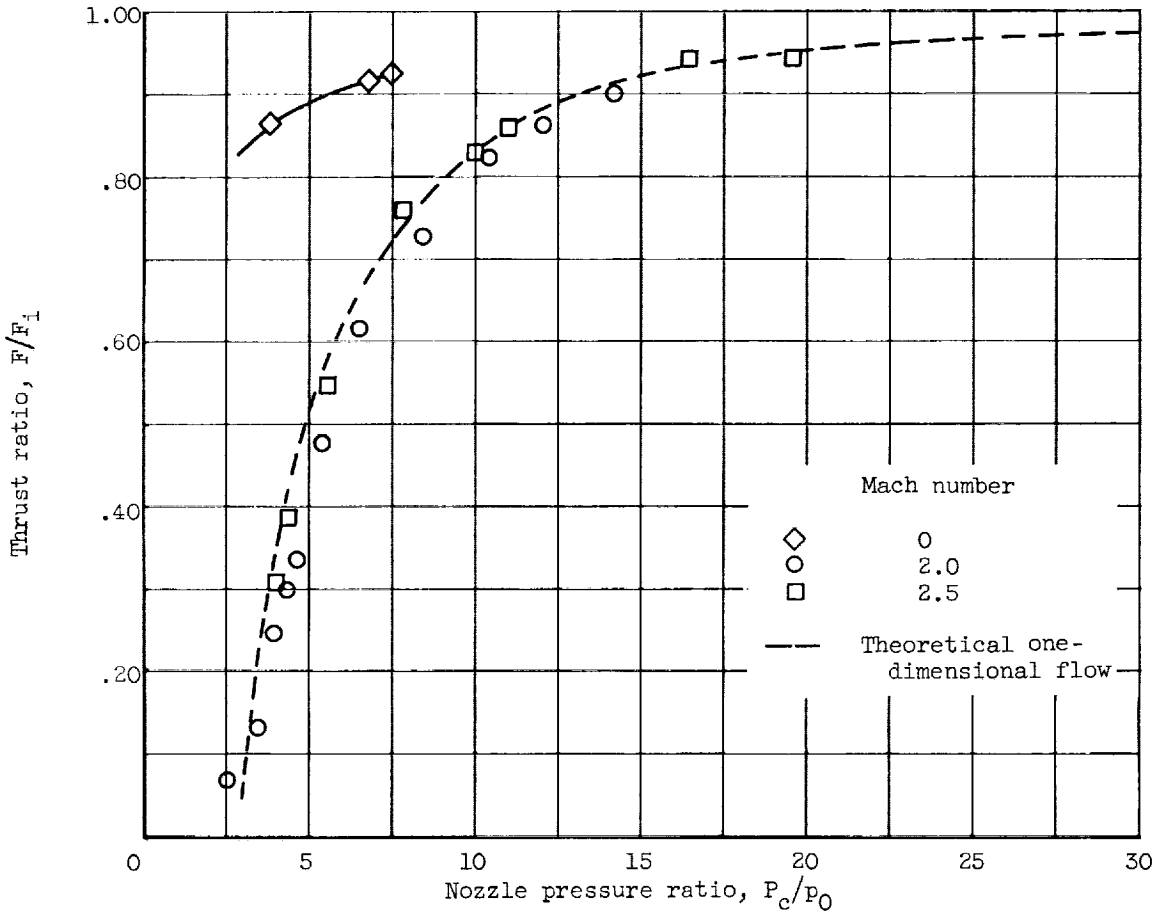

(b) Nozzle area ratio, 6.0.

Figure 5. - Concluded. Variation of thrust ratio with nozzle pressure ratio.

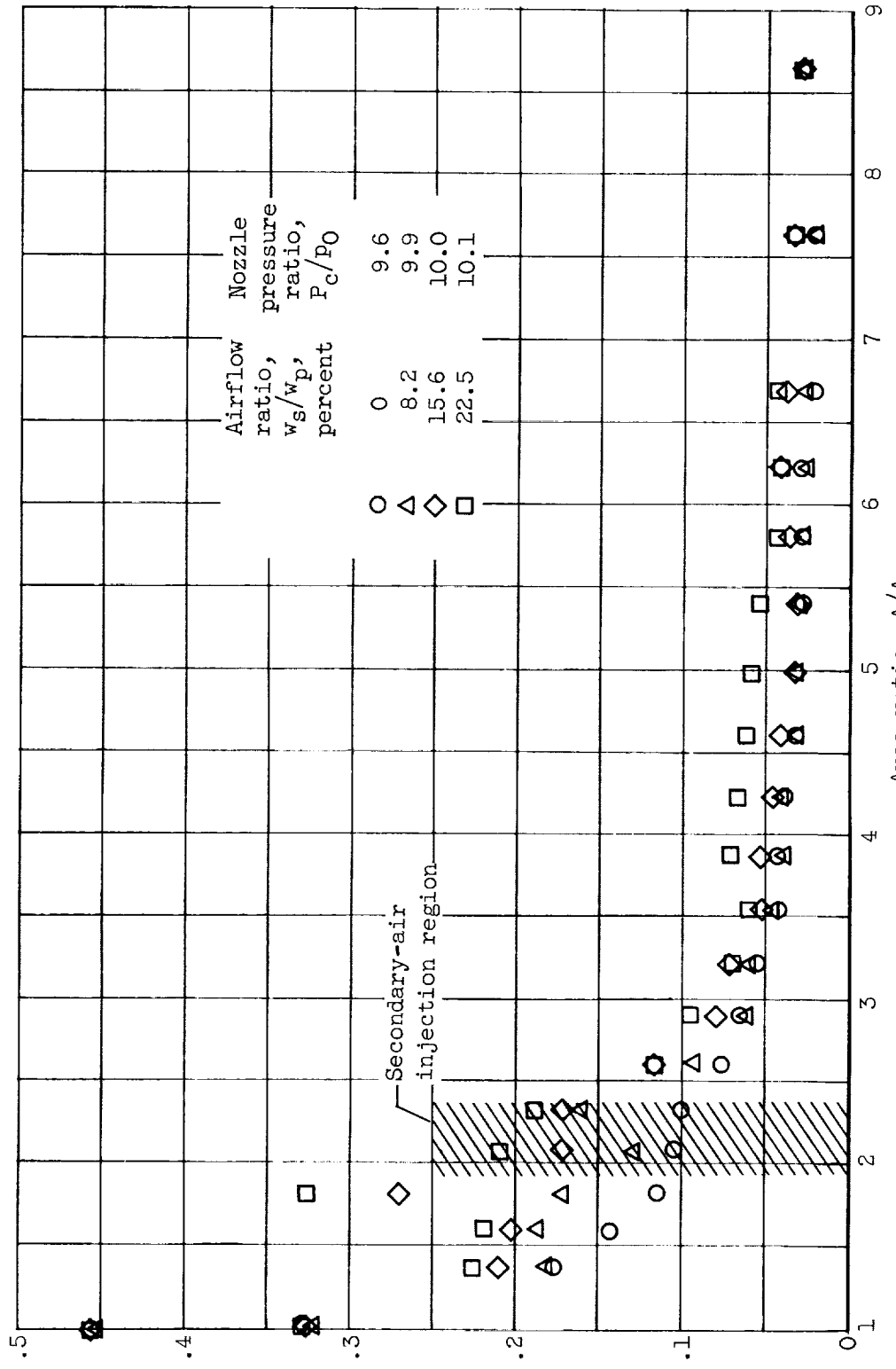

(a) Air injection near the throat.

Figure 6. - Effect of secondary-air injection on nozzle pressure distribution. Free-stream Mach number, 2.5; area ratio 9 nozzle.

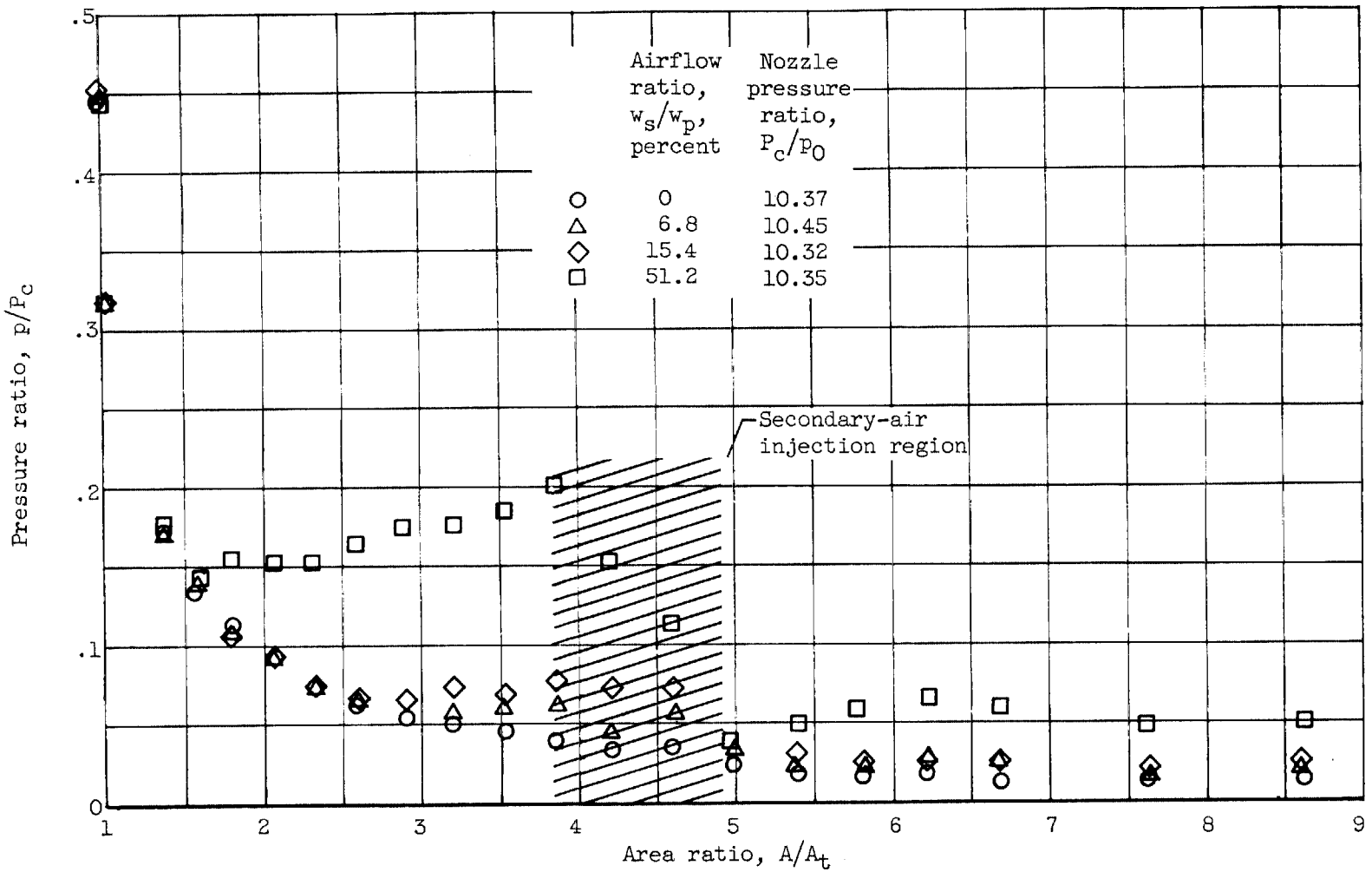

(b) Air injection near nozzle midposition.

Figure 6. - Continued. Effect of secondary-air injection on nozzle pressure distribution. Free-stream Mach number, 2.5; area ratio 9 nozzle.

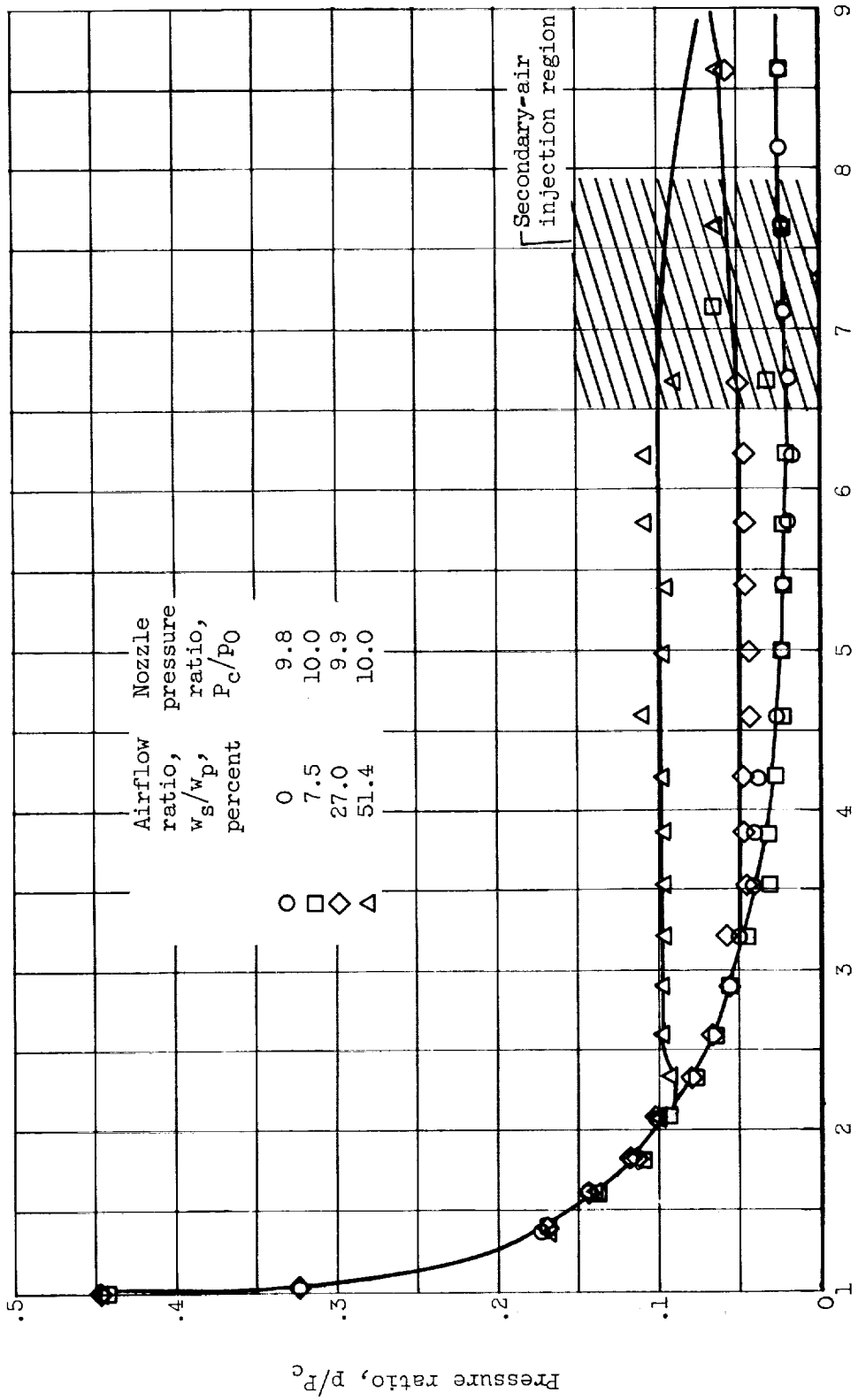

(c) Injection near nozzle exit.

Figure 6. - Concluded. Effect of secondary-air injection on nozzle pressure distribution. Free-stream Mach number, 2.5; area ratio 9 nozzle.

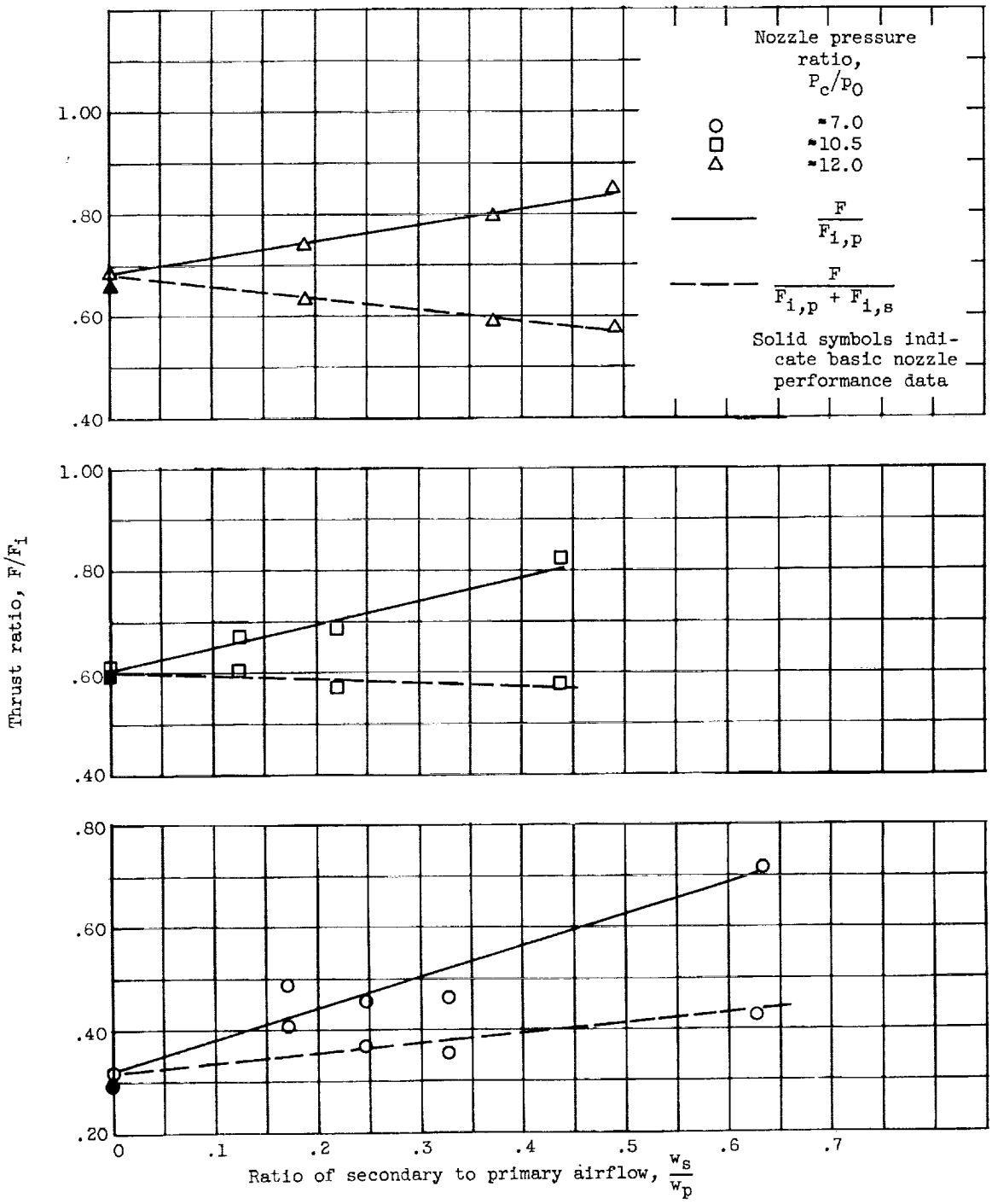

(a) Free-stream Mach number, 2.0.

Figure 7. - Variation of nozzle thrust ratio with secondary airflow. Area ratio 9 nozzle.

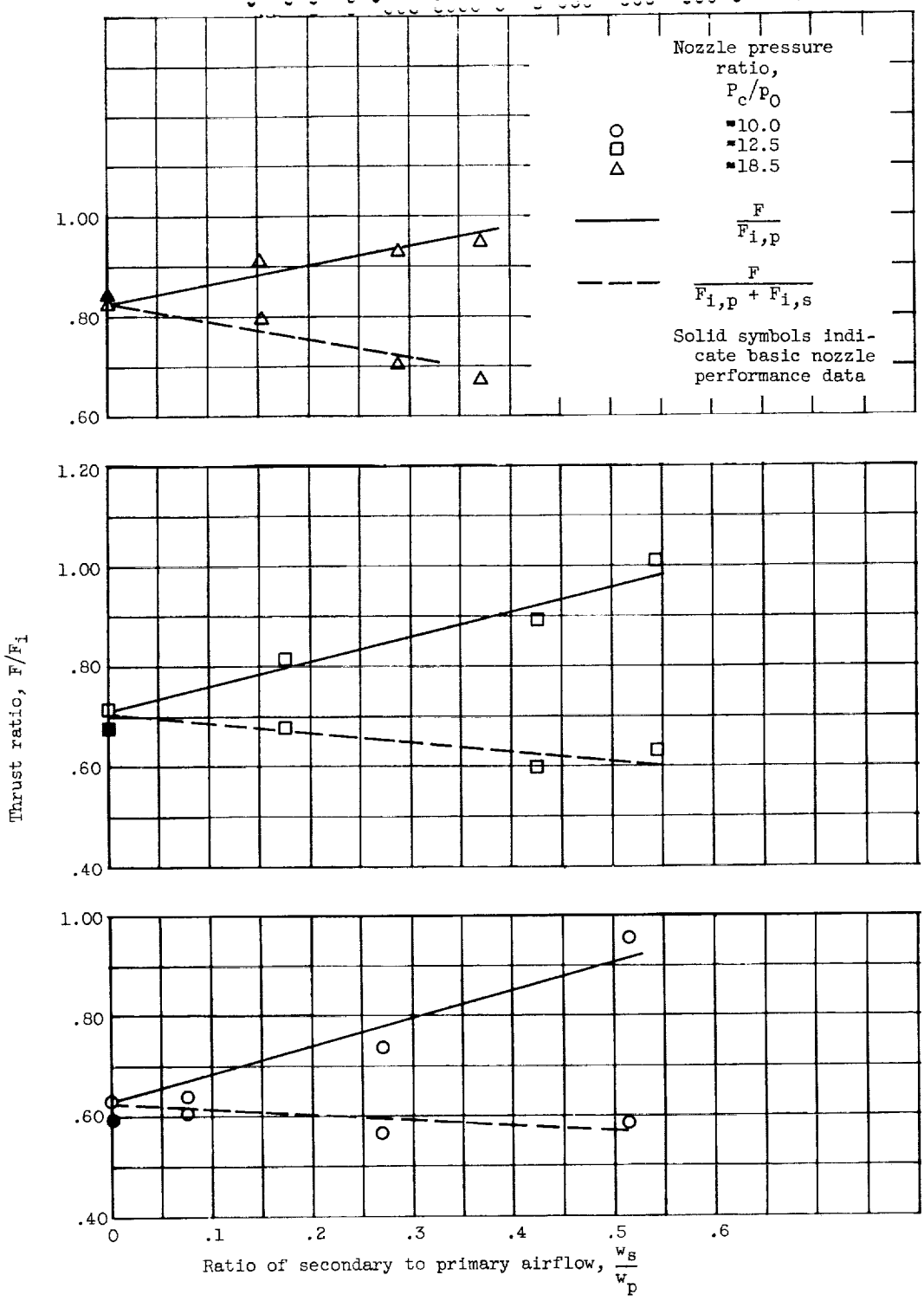

(b) Free-stream Mach number, 2.5.

Figure 7. - Concluded. Variation of nozzle thrust ratio with secondary airflow. Area ratio 9 nozzle.

NASA - Langley Field, Va. E-208